MABS
2021, VOL. 13, NO. 1, e1950264 (14 pages)
https://doi.org/10.1080/19420862.2021.1950264

Taylor & Francis
Taylor & Francis Group

REPORTS

OPEN ACCESS Check for updates

Preclinical evaluation of AFM24, a novel CD16A-specific innate immune cell engager targeting EGFR-positive tumors

Susanne Wingert[a*], Uwe Reusch[a*], Stefan Knackmuss[a], Michael Kluge[a], Michael Damrat[a], Jens Pahl[a], Ute Schniegler-Mattox[a], Thomas Mueller[a], Ivica Fucek[a], Kristina Ellwanger[a], Michael Tesar[a], Torsten Haneke[a], Joachim Koch[a], Martin Treder[b], Wolfgang Fischer[a], and Erich Rajkovic[a]

[a]Research & Development, Affimed GmbH, Heidelberg, Germany; [b]Formerly Affimed GmbH, Heidelberg, Germany. Now: Arjuna Therapeutics, Santiago De Compostela, Spain

ABSTRACT

Epidermal growth factor receptor (EGFR)-targeted cancer therapy such as anti-EGFR monoclonal antibodies and tyrosine kinase inhibitors have demonstrated clinical efficacy. However, there remains a medical need addressing limitations of these therapies, which include a narrow therapeutic window mainly due to skin and organ toxicity, and primary and secondary resistance mechanisms of the EGFR-signaling cascade (e.g., RAS-mutated colorectal cancer). Using the redirected optimized cell killing (ROCK®) antibody platform, we have developed AFM24, a novel bispecific, IgG_1-scFv fusion antibody targeting CD16A on innate immune cells, and EGFR on tumor cells. We herein demonstrate binding of AFM24 to CD16A on natural killer (NK) cells and macrophages with K_D values in the low nanomolar range and to various EGFR-expressing tumor cells. AFM24 was highly potent and effective for antibody-dependent cell-mediated cytotoxicity via NK cells, and also mediated antibody-dependent cellular phagocytosis via macrophages *in vitro*. Importantly, AFM24 was effective toward a variety of EGFR-expressing tumor cells, regardless of EGFR expression level and KRAS/BRAF mutational status. *In vivo*, AFM24 was well tolerated up to the highest dose (75 mg/kg) when administered to cynomolgus monkeys once weekly for 28 days. Notably, skin and other toxicities were not observed. A transient elevation of interleukin-6 levels was detected at all dose levels, 2–4 hours post-dose, which returned to baseline levels after 24 hours. These results emphasize the promise of bispecific innate cell engagers as an alternative cancer therapy and demonstrate the potential for AFM24 to effectively target tumors expressing varying levels of EGFR, regardless of their mutational status.

Abbreviations: ADA: antidrug antibody; ADCC: antibody-dependent cell-mediated cytotoxicity; ADCP: antibody-dependent cellular phagocytosis; AUC: area under the curve; CAR: chimeric-antigen receptor; CD: Cluster of differentiation; CRC :colorectal cancer; ECD: extracellular domain; EGF: epidermal growth factorEGFR epidermal growth factor receptor; ELISA: enzyme-linked immunosorbent assay; FACS: fluorescence-activated cell sorting; Fc: fragment, crystallizableFv variable fragment; HNSCC: head and neck squamous carcinomalL interleukinm; Ab monoclonal antibody; MOA: mechanism of action; NK :natural killer; NSCLC: non-small cell lung cancer; PBMC: peripheral blood mononuclear cell; PBS: phosphate-buffered saline; PD: pharmacodynamic; ROCK: redirected optimized cell killing; RSV: respiratory syncytial virus; SABC: specific antibody binding capacity; SD: standard deviation; TAM: tumor-associated macrophage; TKI: tyrosine kinase inhibitor; WT: wildtype

ARTICLE HISTORY
Received 23 December 2020
Revised 14 June 2021
Accepted 28 June 2021

KEYWORDS
Protein engineering; antibody therapy; FCVR; innate immunity; antibody-dependent cellular cytotoxicity (ADCC); antibody-dependent cellular phagocytosis (ADCP); EGFR targeting; immuno-oncology; solid tumors

Introduction

The epidermal growth factor receptor (EGFR) is a transmembrane glycoprotein belonging to the erbB family of tyrosine kinase receptors.[1] Binding of EGFR to its ligands leads to activation of signal transduction pathways that are involved in regulating cellular proliferation, differentiation, and survival.[1] Although also expressed by normal cells, EGFR is overexpressed in many solid tumors, including colorectal cancer (CRC), head and neck squamous cell carcinoma (HNSCC), and non–small cell lung cancer (NSCLC), and has been associated with poor prognosis and decreased survival.[1] Multiple ligands bind to and activate EGFR, including amphiregulin, epiregulin, epidermal growth factor (EGF), and transforming growth factor-α.[1,2] Ligand binding results in an extended conformation of the extracellular domain (ECD), which then promotes EGFR homo- or heterodimerization and a conformational change of the receptor resulting in the autophosphorylation of the intracellular tyrosine kinase domains. Phosphotyrosine residues then activate, either directly or through adaptor proteins, downstream components of signaling pathways including Ras/MAPK, PLCγ1/PKC, PI3 kinase/Akt, and STAT pathways.[1,3,4]

Two major classes of drugs targeting the inhibition of EGFR signal transduction have been developed: (1) anti-EGFR monoclonal antibodies (mAbs), such as cetuximab and panitumumab, which inhibit ligand binding by preventing the

CONTACT Erich Rajkovic E.Rajkovic@affimed.com Affimed GmbH, Heidelberg, Germany
*Authors contributed equally
Supplemental data for this article can be accessed on the publisher's website

receptor from adopting the extended conformation required for dimerization,[3] and (2) tyrosine kinase inhibitors (TKIs) such as gefitinib, erlotinib, and Osimertinib, which act by competitively binding to the intracellular ATP pocket of the EGFR kinase domain. Cetuximab (an IgG_1) and panitumumab (an IgG_2) are indicated for different treatment regimens limited to CRC and HNSCC; however, response rates and improvements in overall survival have been modest,[5–7] and many patients fail to respond to these therapies.[8] Both antibodies bind with high specificity to the ECD of EGFR and inhibit ligand binding and downstream signaling.[5,9,10] This mechanism of action (MOA) is ineffective in tumors carrying KRAS mutations (~40% of patients with CRC).[11] Importantly, skin toxicity is common in the majority of patients (45–100%) receiving EGFR-targeted therapy.[12] A second potential, less pronounced MOA for IgG_1 mAbs such as cetuximab involves engagement of immune effector cells expressing the Fcγ receptor IIIA (CD16A) on natural killer (NK) cells, triggering antibody-dependent cell-mediated cytotoxicity (ADCC).[13–15] The Fc region of mAbs binds to CD16A on NK cells and myeloid cells.[16]

Second-generation antibodies that augment ADCC have been created by incorporating Fc-enhanced properties.[5,17,18] GA201 (imgatuzumab, RO5083945) was the first humanized IgG_1 anti-EGFR mAb that demonstrated enhanced ADCC via altered glycosylation of the Fc region.[17] GA201 showed clinical efficacy at high doses in a Phase 1/2 trial and was tested in combination with cetuximab for clinical efficacy for HNSCC and *in vitro* for NSCLC.[5,18,19] However, GA201 is no longer in active clinical development. Tomuzotuximab, a glycoengineered antibody of cetuximab, was optimized at its Fc domain to improve efficacy and reduce side effects.[20] In a Phase 1 study in patients with solid tumors, it was found safe, well tolerated and showed clinical activity. The most frequent drug-related adverse events were infusion-related reactions (76%) and skin toxicity (73%).[20] A Phase 1b trial of tomuzotuximab in combination in solid tumors has just recently completed its recruitment (NCT03360734). Fc-optimized mAbs may target a wider population, replacing the parent antibody in combination therapies.[20]

The EGFR TKIs are small-molecule inhibitors that prevent tyrosine phosphorylation of the intracellular kinase domain and subsequent activation of signal transduction pathways. The two most common types of EGFR-activating mutations are small deletions and amino acid substitutions, which collectively account for >90% of known activating EGFR mutations, conferring sensitivity to EGFR-TKI therapy, resulting in higher response rates (up to 70%) and longer median survival than those observed in patients with wild-type (WT) EGFR.[21,22] Greater treatment sensitivity is a result of increased affinity of the ATP-binding pocket for EGFR TKIs as compared with WT EGFR.[23] Regardless, most patients with EGFR-mutant NSCLC and treated with EGFR TKIs develop resistance within 9–14 months. Patients who initially respond to first-generation gefitinib or erlotinib can acquire secondary EGFR mutations (acquired resistance), such as the T790M mutation, which accounts for about half of the cases of EGFR mutations after disease progression.[23,24] Third-generation TKI inhibitors, e.g., osimertinib, can overcome such secondary acquired resistances, in particular the T790M resistance. However, recent data suggest the occurrence of multiple resistance mechanisms even for osimertinib treatment.[25] Although EGFR mAbs and TKIs show promise, dose-limiting toxicities, such as skin rash have been observed.[26] Therefore, there remains an unmet medical need for patients suffering from EGFR-expressing cancers who are not benefitting from current EGFR-targeted therapies.

NK cells are cytotoxic lymphocytes of innate immunity and are essential for immunosurveillance of infections and cancer.[27] CD16A is the main Fc receptor expressed by human NK cells and induces activation signals and killing of target cells opsonized by antibodies via ADCC,[16] characterized by release of cytotoxic granules, death receptor signaling, and release of pro-inflammatory cytokines.[28] Macrophages are prevalent in many types of solid tumors (breast, lung, colorectal, and melanoma) as tumor-associated macrophages (TAM), that promote tumor angiogenesis and suppress antitumor immune mechanisms.[29] However, TAMs can also either antagonize, augment, or mediate the antitumor effects of cytotoxic agents, tumor irradiation, and checkpoint inhibitors.[30–32] Furthermore, macrophages have immense potential to destroy tumor cells via antibody-dependent cellular phagocytosis (ADCP).[33,34]

Immunotherapeutic approaches targeting and engaging innate immune cells for anti-cancer therapy have shown clinical efficacy combined with a favorable safety profile, as demonstrated by adoptive transfer of activated[35] or cytokine-induced memory-like NK cells in myeloid leukemia.[36] Importantly, the first clinical trial on NK cells expressing a chimeric antigen receptor (CAR) targeting CD19 has shown encouraging efficacy without major toxicity.[37] Most recently, first preclinical data on CAR macrophages targeting several tumor antigens have demonstrated efficacy in preclinical studies.[38] In addition, numerous bispecific antibodies targeting NK cells are in development.[39] The most clinically advanced innate immune cell engager is a bispecific, tetravalent antibody that targets CD30 and CD16A, referred to as AFM13.[40,41] AFM13 has been assessed as monotherapy in a dose-escalating Phase 1 clinical study, as well as in combination with pembrolizumab in patients with Hodgkin lymphoma.[41,42]

Here, AFM24, a bispecific, tetravalent antibody, targeting EGFR on tumor cells and CD16A on innate immune cells, i.e., NK cells and macrophages, is described. We demonstrate the *in vitro* binding capability of AFM24 to different tumor cell lines expressing varying levels of EGFR. Functionally, we test the potency and ability of AFM24 to mediate tumor cell depletion via ADCC or ADCP, by NK cells or macrophages, respectively. AFM24 was administered to cynomolgus monkeys to determine the safety and tolerability profile *in vivo*, pharmacokinetic and pharmacodynamic parameters.

Results

AFM24 design and biochemical characterization

Using the ROCK® platform, AFM24 is designed as a tetravalent bispecific IgG_1-single-chain variable fragment (scFv) fusion antibody (scFv-IgAb) specific for human EGFR and CD16A

(Figure 1).[43] The CD16A-specific human IgG_1 is connected to anti-EGFR scFvs fused to the C-terminus of each heavy chain. Amino acid substitutions were introduced to abolish Fc-mediated effector functions of human IgG_1. The EGFR-specific single-chain variable domains consist of one VH and one VL domain fused to the C-terminus of the IgG heavy-chain CH3 domains via a flexible peptide linker sequence (connector). Each VH and VL domain of both scFv are connected to each other via a flexible peptide linker sequence (linker) (Figure 1). AFM24 is designed such that the Fv domains for each specificity preferentially bind in cis, i.e., bivalently to CD16A on NK cells and bivalently to EGFR on target cells, and trans-binding is only intended for crosslinking of $CD16A^+$ effector cells with $EGFR^+$ target cells to trigger target cell killing.[43] HPLC-analyzed product (Supplementary Fig. S1A) and SDS-PAGE analysis confirms sample purity and integrity of both AFM24 polypeptide chains (Supplementary Fig. S1B). Under non-reducing conditions, AFM24 migrates as a single band (>200 kDa) with a predicted MW of 196 kDa. Under reducing conditions, two protein bands migrating at ~81 kDa and ~27 kDa apparently represent the heavy chain and light chain of AFM24 with a predicted MW of 75.5 kDa and 22.6 kDa, respectively (Supplementary Fig. S1B).

Characterization of AFM24 binding to human NK cells and macrophages via CD16A

To determine AFM24 binding specificity and apparent affinity for CD16A-positive immune effector cells, either human NK cells or macrophages were combined with increasing concentrations of AFM24 and control antibodies at 37°C before binding was measured by flow cytometry to calculate K_D values by non-linear regression (Figure 2 A and B). To demonstrate that AFM24 binds to a specific epitope on CD16A distinct from the Fc binding site, AFM24 binding was tested on NK cells in the presence or absence of physiological concentrations (10 mg/mL) of polyclonal human serum IgG. AFM24 bound to NK cells with high affinity (mean K_D, 6.2 ± 2.0 nM) in the absence of competing IgG. The addition of polyclonal IgG resulted in only a slight decrease (1.9-fold loss in K_D) in binding (mean K_D, 11.8 ± 4.3 nM) (Figure 2a). This observation strongly suggests that AFM24 binds to a distinct region on CD16A on NK cells that does not overlap with the Fc binding site. In contrast to AFM24, high affinity binding of Fc-enhanced anti-EGFR IgG_1 was significantly inhibited in the presence of polyclonal IgG binding. AFM24 specifically binds to CD16A with negligible binding to other Fcγ receptors (CD32, CD64), and lack of binding to CD16B (FcγRIIIB) due to negative selection during screening for scFvs.[40,43] Binding of AFM24 to primary human CD16A-expressing macrophages (mean K_D, 13.4 ± 11.2 nM) was confirmed on macrophages derived from five different individual healthy donor peripheral blood mononuclear cells (PBMC) (Figure 2b). Substantial higher apparent affinity of AFM24 for CD16A compared to a monovalent anti-CD16A construct (185.2 nM, data not shown) suggests that AFM24 preferentially binds bivalently to $CD16A^+$ cells in cis.

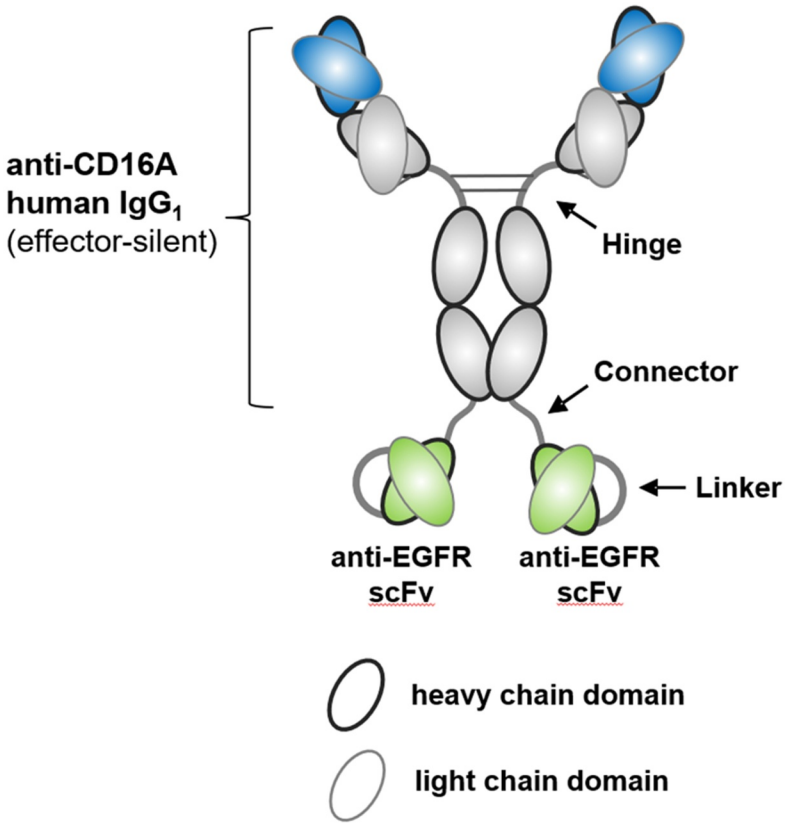

Figure 1. AFM24 structural model. AFM24 is a tetravalent bispecific IgG_1-scFv fusion antibody (scFv-IgAb) specific for human EGFR and human CD16A with silenced IgG_1 Fc.

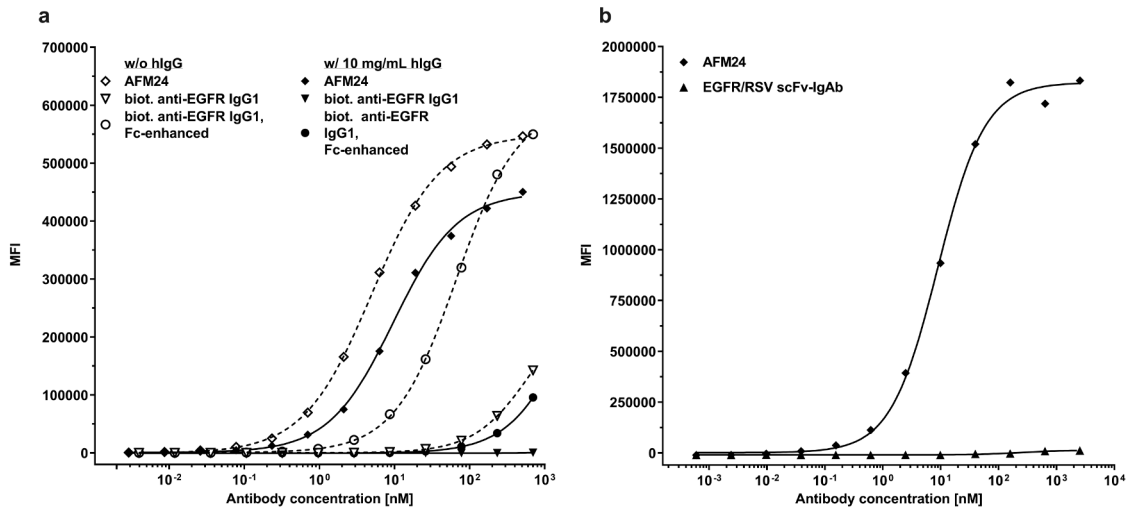

Figure 2. High affinity binding of AFM24 to CD16A-expressing effector cells *in vitro*. A) Binding of AFM24, biotinylated human IgG_1 anti-EGFR, and biotinylated Fc-enhanced IgG_1 anti-EGFR to enriched primary human NK cells was assessed by flow cytometry in the presence (open symbols) or absence (filled symbols) of 10 mg/mL polyclonal human serum IgG at 37°C. One representative experiment is shown out of seven performed. B) Binding of AFM24 and the negative control antibody (EGFR/RSV scFv-IgAb) was assessed by flow cytometry on *in vitro* differentiated human macrophages. One representative experiment is shown out of seven performed. Biot., biotinylated, MFI, median fluorescence intensity.

AFM24 binding to tumor cell lines with different levels of EGFR expression

The apparent binding affinities of AFM24 at 37°C on various tumor cell lines of different origins with different EGFR expression levels was determined (Figure 3, Supplementary Table S1). AFM24 binds to EGFR-positive tumor cells with affinities in the nanomolar range (<100 nM), with the highest affinity for DK-MG glioma cells (2.6 ± 1.2 nM) and relatively lower affinity for HCT-116 cells (89.8 ± 63 nM) (Figure 3, Supplementary Table S1). Cell lines with lower EGFR expression resulted in lower apparent affinities, with undetectable AFM24 binding for the very low EGFR-expressing cell line MCF-7. Collectively, AFM24 binding affinity generally correlates with EGFR expression level of the respective cell lines (Spearman coefficient, r = −0.7133, p = .0118), suggesting that bivalent binding is not supported on target cell lines showing low EGFR density levels. On target cell lines with high expressing levels of EGFR AFM24 exhibits substantial higher apparent affinities (8.1 nM on A-431) than a monovalent anti-EGFR scFv (mean K_D on A-431: 62.6 nM). Taken together, the results describe AFM24 binding to various EGFR-positive cell lines over a wide range of EGFR expression levels.

AFM24-mediated ADCC by human NK cells on tumor cell lines in vitro

To test for AFM24 functionally, *in vitro* ADCC was measured in cytotoxicity assays with PBMC-derived human NK cells cultured with calcein-labeled tumor target cell lines and increasing concentrations of AFM24 and EC_{50} (potency) and E_{max} (efficacy) values were determined. AFM24 induced potent ADCC on 11 tumor cell lines of different origins, representing a wide range of EGFR surface expression (Table 1, Supplementary Fig. S2). The potency of AFM24 ranged from 0.7 ± 0.4 pM (DK-MG cells) to 47.7 ± 19.0 pM (SW-982 cells) with a lack of correlation between potency and EGFR expression level (SABC) (Spearman coefficient, r = −0.3326, p = .3158). The efficacy of AFM24 ranged from 92.9 ± 19.3% (DK-MG cells) to 21.2% (LoVo cells) with a lack of correlation between efficacy and SABC (Spearman correlation, r = 0.3636, p = .2731). AFM24 induced ADCC-

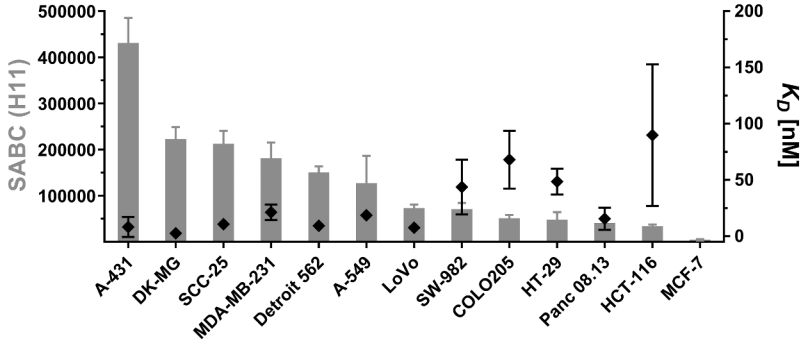

Figure 3. Mean specific antibody binding capacity (SABC) and mean apparent binding affinities of AFM24 on tumor cell lines with different levels of EGFR expression. Mean EGFR densities (SABC) determined with anti-EGFR antibody (clone H11) on various tumor cell lines (left Y-axis) were plotted against mean apparent binding affinities (K_D, right Y-axis). Error bars represent SD (SABC, $n \geq 3$ independent experiments; apparent affinity (K_D), $n \geq 2$ independent experiments). Values depicted are listed in Supplementary Table S1.

Table 1. AFM24-mediated ADCC by NK cells on various tumor cell lines *in vitro*.

			SABC (H11)		EC_{50} [pM]		E_{max} [%]	
Cell line	Indication/ origin	Mutation in KRAS/BRAF genes	Mean	SD	Mean	SD	Mean	SD
MCF-7	Breast	None	4,546	1,689	20.9	1.6	34.6	13.6
MDA-MB-231	Breast	BRAFG464V, KRASG13D	181,487	33,939	5.5	n/a	57.1	n/a
COLO205	CRC	BRAFV600E	51,177	7,307	30.4	25.7	50.7	11.9
HT-29	CRC	BRAFV600E, T119S	48,174	16,571	4.2	2.2	49.8	1.0
LoVo	CRC	KRASG13D	73,187	7,648	3.9	n/a	21.2	n/a
DK-MG	Glioma	None	222,648	26,148	0.7	0.4	92.9	19.3
Detroit 562	HNSCC	None	150,464	13,150	3.9	1.0	67.5	2.9
SCC-25	HNSCC	None	212,477	28,260	23.5	16.3	42.0	16.5
Panc 08.13	Pancreas	KRASG12D	40,913	7,279	4.6	2.2	45.3	14.4
SW-982	Sarcoma	BRAFV600E	71,006	13,506	47.7	19	83.5	11.4
A-431	Squamous carcinoma	None	431,125	54,336	1.8	1.5	58.2	17.3

Specific antibody binding capacity (SABC) was determined in ≥3 independent experiments. Potency (EC_{50}) and efficacy (E_{max}) for AFM24 was determined in 1–4 independent experiments.

CRC, colorectal cancer; HNSCC, head and neck squamous cell carcinoma; SD, standard deviation; EC_{50}, half maximal effective concentration; E_{max}, maximal observed efficacy; n/a, not applicable.

mediated depletion of target cells independent of their KRAS/BRAF mutation status *in vitro* (Table 1). Surprisingly, although the apparent binding affinity of AFM24 could not be calculated for the very low EGFR-expressing breast cancer cell line MCF-7 cells due to the lack of detectable AFM24 binding (Figure 3 and Supplementary Table S1), potent (picomolar range) AFM24-mediated ADCC could still be detected (Table 1). Interestingly, while this data may indicate a correlation of the apparent affinity of AFM24 to tumor cell lines and EGFR expression, no correlation between EGFR expression and AFM24 potency and efficacy in ADCC assays could be observed. These results suggest that two valencies for CD16A and high apparent affinity for NK cells are advantageous for triggering NK cell-mediated lysis of target cells expressing lower numbers of EGFR antigens. On the other hand, increasing EGFR expression levels did not lead to higher potency or efficacy of AFM24, which might be due to maximal stimulation of NK cells by AFM24 at the used E:T ratios in the experimental setting. Of note, this effect was previously shown with other ROCK ® molecules.[43] Lastly, AFM24-mediated ADCC was dependent on the presence of EGFR on target cells, as AFM24 did not induce lysis of the EGFR-negative KARPAS-299 tumor cell line by NK cells (Supplementary Fig. S2). Taken together, these results show the high potency of AFM24-mediated ADCC in the picomolar range against a wide selection of tumor cell lines of different origins, characterized by a broad range of EGFR surface expression levels and different KRAS/BRAF mutational status.

AFM24 demonstrates sustained cytotoxic potential in the presence of competing serum IgG

An important question is whether the serum IgG pool in peripheral blood competes for CD16A binding on human NK cells, thereby reducing the potency and efficacy of AFM24. To this end, we used the sarcoma cancer cell line SW-982 in an ADCC assay with 10 mg/mL of the monoclonal anti-respiratory syncytial virus (RSV) IgG_1 (palivizumab) as a surrogate for circulating IgG (Figure 4a). This ADCC assay was performed with monoclonal IgG_1 in lieu of polyclonal serum IgG, since it was shown that polyclonal serum IgG preparations interfere with the ADCC assay.[43] The efficacy of cetuximab in ADCC, as determined by the maximal lysis of tumor cells (E_{max}), decreased 2.6-fold in the presence of competing IgG, whereas AFM24 was only marginally affected (1.3-fold) (Supplementary Table S2). These data demonstrate that AFM24-engaged NK cells can mediate efficient tumor cell elimination in the presence of circulating IgG *in vitro*.

AFM24-induced ADCC at low effector-to-target ratios

To assess how the effector-to-target (E:T) ratio affects AFM24-mediated ADCC, we performed calcein-release assays with enriched primary human NK cells and Panc 08.13 as target cells with varying E:T ratios at a fixed concentration of AFM24, negative control antibodies targeting the irrelevant RSV antigen, and cetuximab (Figure 4b). ADCC activity with AFM24 on Panc 08.13 resulted in complete lysis at the two highest E:T ratios (30:1, 20:1), while at the highest E:T ratio (30:1), cetuximab induced a mean tumor cell lysis of 74.9%. AFM24 was able to induce tumor cell lysis at an E:T ratio as low as 0.3:1 and generally demonstrated higher activity compared to cetuximab in two independent experiments at low E:T ratios (Supplementary Table S3). Antibody-mediated target cell lysis was not observed in the presence of the RSV-targeting control antibody constructs (RSV/CD16A, EGFR/RSV) comprising the same antibody scaffold as AFM24, but each lacking either the EGFR- or the CD16A-binding domains (Figure 4b). This observation clearly demonstrates that both specificities of AFM24 are required for effective lysis, and that binding of RSV/CD16A scFv-IgAb to CD16A alone does not enhance the natural cytotoxicity of NK cells toward tumor target cells. In summary, AFM24 mediated potent and efficacious target cell lysis even at low E:T ratios, suggesting efficient effector cell engagement and efficacy in tumors characterized by low numbers of intra-tumoral NK cells.

AFM24-induced ADCP of high- and low-expressing EGFR tumor cells by macrophages

AFM24-mediated ADCP activity by *in vitro* differentiated human macrophages was assessed using $EGFR^{high}$-expressing DK-MG, $EGFR^{int}$-expressing A-549 and SW-982, and $EGFR^{low}$-expressing HCT-116 target cells. Of note, HCT-116 harbors the KRASG13D gene mutation, resulting in constitutively active RAS/RAF/MAPK signaling.[44] ADCP was measured by co-culturing human

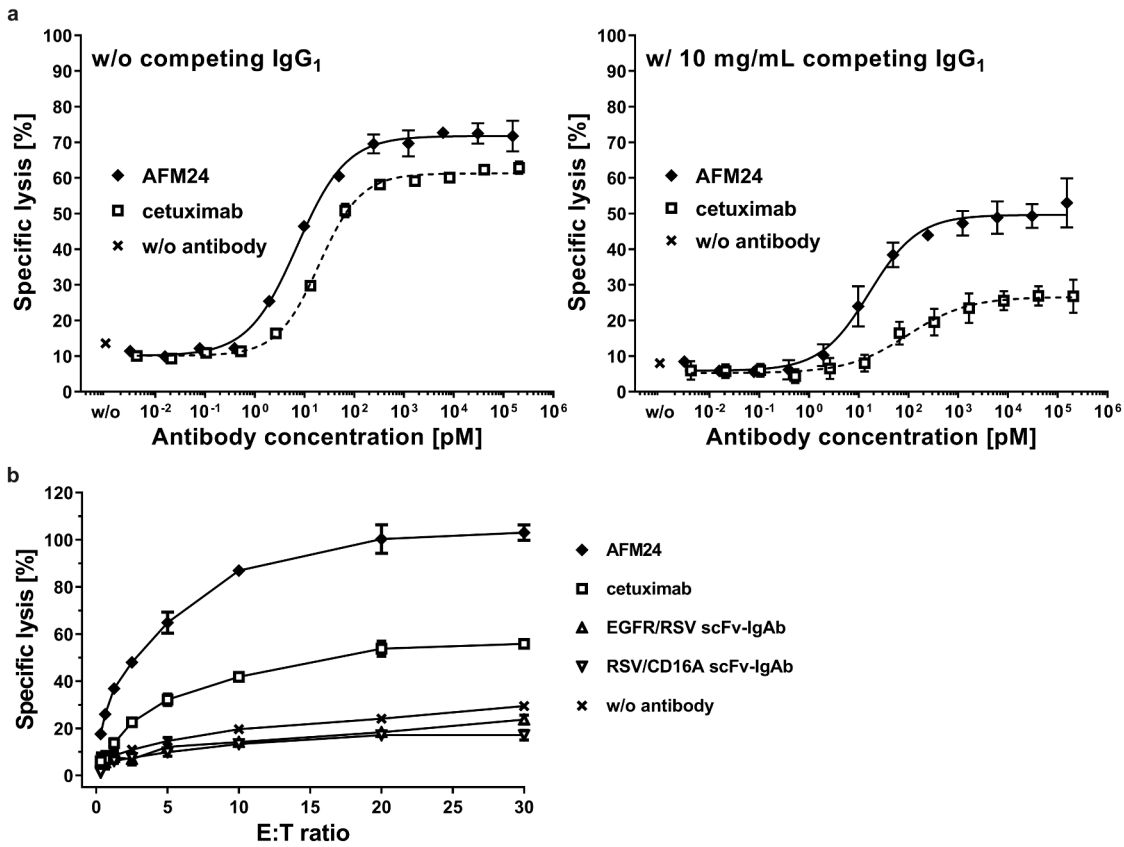

Figure 4. AFM24 retains high ADCC activity in the presence of competing IgG and at low effector-to-target (E:T) ratio. A) Comparison of AFM24- and cetuximab-mediated ADCC in the presence or absence of competing IgG *in vitro* in 4 h calcein-release cytotoxicity assays with EGFR-positive SW-982 target cells and primary human NK cells as effector cells at an E:T ratio of 5:1 with or without AFM24 or cetuximab. Assays were performed in the presence or absence of 10 mg/mL anti-RSV IgG_1 palivizumab. B) Lysis of Panc 08.13 target cells was determined in a 4 h calcein-release assays with primary human NK cells as effector cells at increasing E:T ratios in the presence of 5 µg/mL AFM24, cetuximab, EGFR/RSV and RSV/CD16A control scFv-IgAbs, or without antibody. One representative experiment out of two is shown for each figure. Error bars represent SD.

macrophages with fluorescent-labeled tumor cells and analyzing tumor cell uptake (phagocytosis) by macrophages (Supplementary Figure S3). AFM24 induced robust macrophage-mediated ADCP of $EGFR^{high}$ and $EGFR^{low}$ target cells (Figure 5). In contrast, cetuximab was only effective with the $EGFR^{high}$ cells and failed to mediate ADCP toward $EGFR^{int}$ and $EGFR^{low}$ target cells. The AFM24-induced increase in ADCP versus controls (no antibody) was 7.1- and 11.7-fold in DK-MG and HCT-116 cells, respectively. The increase in ADCP of HCT-116 cells observed with cetuximab was only 1.7-fold. Negative control antibodies, anti-RSV/CD16A and anti-EGFR/RSV, did not induce ADCP, demonstrating the requirement for AFM24 to bind both the macrophages and tumor cells. Taken together, these data suggest efficient AFM24-mediated phagocytosis of EGFR-expressing tumor cells by ADCP and appears to be unrelated to EGFR-expression levels or the KRAS mutational status of the target cells.

Effect of AFM24 on EGFR signaling in human tumor cell lines

Signal transduction inhibition of the EGFR pathway is frequently associated with dermatologic toxicities such as skin rash.[45] Therefore, we assessed the potential of AFM24 to inhibit EGF-induced signaling. AFM24 reduced EGF-mediated EGFR phosphorylation in a dose-dependent manner on two different tumor cell lines, A-431 and A-549 (Figure 6). However, complete inhibition of EGFR phosphorylation at concentrations up to 5 mg/mL (~25 µM) could only be observed for A-549, but not for A-431 tumor cells (Figure 6). For A-549 tumor cells, AFM24 and anti-EGFR/RSV were able to fully inhibit EGFR-phosphorylation at concentrations of 532.0 µg/mL (2.7 µM) and 662.6 µg/mL (3.4 µM) and IC_{50} values of 430 µg/mL (2.2 µM) and 630.9 µg/mL (3.2 µM), respectively (Figure 6 B). As expected, no inhibition was observed with the control antibody RSV/CD16A, demonstrating that the observed inhibition of AFM24 is exclusively due to the EGFR-targeting domains. In contrast to AFM24, treatment with cetuximab led to full inhibition of EGFR phosphorylation on both A-431 and A-549 cells, with IC_{50} of 6.3 µg/mL (0.04 µM) and 0.2 µg/mL (1 nM), respectively. In conclusion, AFM24 has the capability to inhibit EGF-stimulated EGFR-phosphorylation on A-431 and A-549 cells *in vitro* only at very high antibody concentrations. The differences in affinity of AFM24 on A-431 cells (mean K_D: 8.1 nM) and on A-549 cells (mean K_D: 18.6 nM) compared to cetuximab (mean K_D on A-431: 2.2 nM; mean K_D on A-549: 0.2 nM) may contribute to the lower signaling inhibition. The epitope on EGFR for AFM24 that could also result in differences in signaling inhibition is not yet determined. Binding assays on cells and recombinant EGFR demonstrate competition between AFM24 and

cetuximab on EGFR suggesting overlapping epitopes or sterical interference of the two antibody constructs (Supplementary Figure S4). Compared to cetuximab, the inhibitory activity of AFM24 is >1000-fold lower, which implies a favorable safety profile of AFM24 over cetuximab *in vivo*.

Toxicology and pharmacokinetic data in cynomolgus monkeys

To advance AFM24 into clinical development, the safety of AFM24 in cynomolgus monkeys was determined in a 28-day toxicity study with repeated intravenous infusion (2-hour infusion, once a week) followed by a 28-day recovery phase to detect potentially delayed toxicity and to assess the reversibility of the potential effects observed. A total of 36 monkeys (18 males and 18 females) were allocated to 4 dose groups (vehicle, 8, 24, and 75 mg/kg/week five doses in total); the study design is summarized in Supplementary Table S4. No AFM24-related findings in clinical signs, body weights, food consumption, body temperature, cardiovascular investigations, ophthalmology, clinical chemistry, hematology, coagulation, urinalysis, or anatomic pathology were detected.

Toxicokinetic parameters were assessed by non-compartmental analysis. The observed increases in AFM24 exposure, as assessed by mean C_{max} and $AUC_{0\text{-}168}$ (Area under the curve) values, were proportional to the increases of

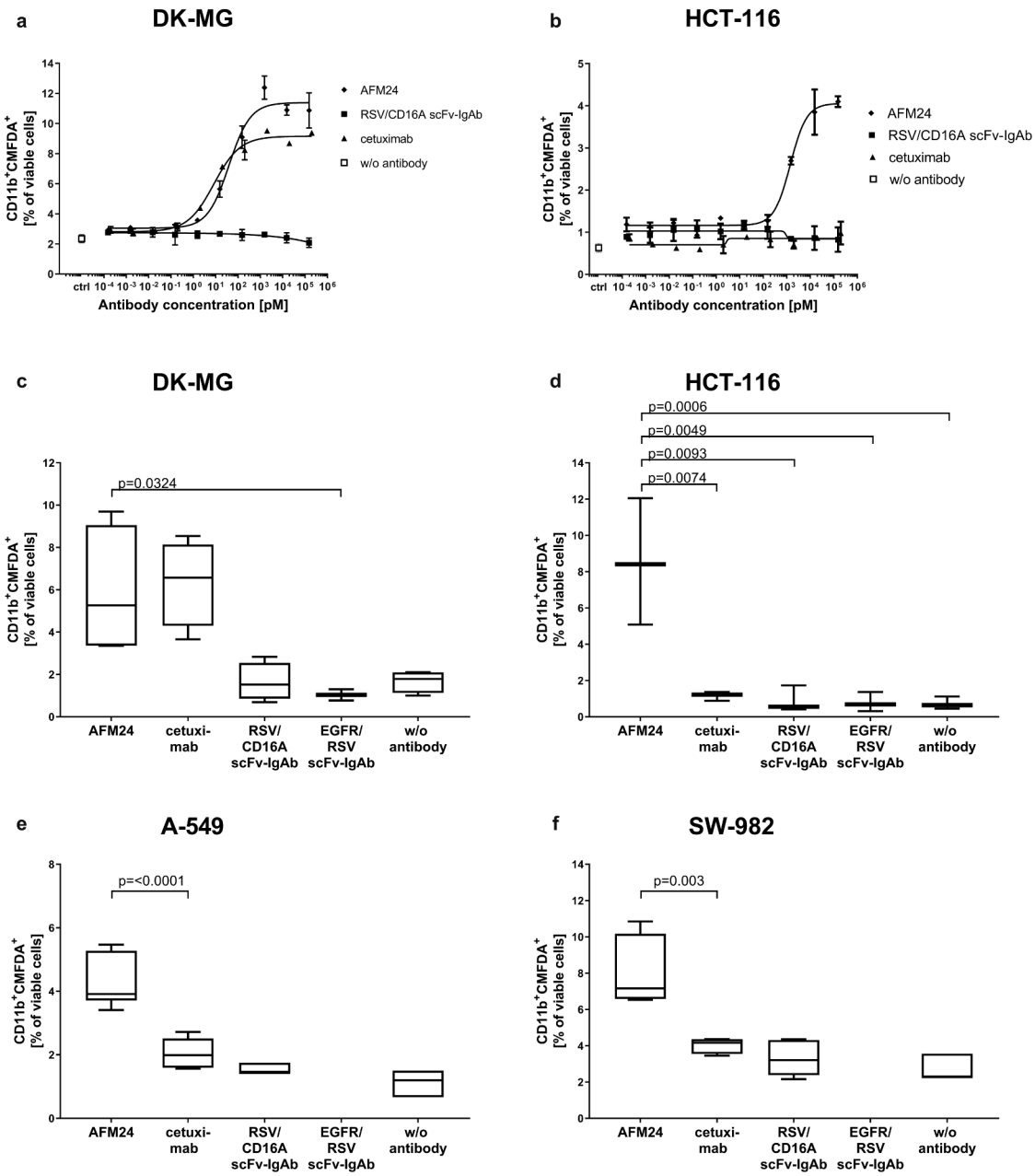

Figure 5. AFM24-induced ADCP toward EGFR-expressing tumor cells by macrophages after co-culture for 4 hours at an E:T ratio of 5:1. Concentration-dependent ADCP by AFM24, control antibody or cetuximab of $EGFR^{high}$ expressing DK-MG target cells (a) and $EGFR^{low}$ expressing HCT-116 target cells (b). One representative experiment is shown. Error bars represent the SD. ADCP at fixed antibody concentration of $EGFR^{high}$ DK-MG (at 10 µg/mL) (c), $EGFR^{int}$ A-549 (at 30 µg/mL) (e) as well as $EGFR^{low}$ HCT-116 (at 10 µg/mL) (d) and SW-982 (30 µg/mL) (f) target cells. Data were combined of three to six experiments depicted as box plot with median and whiskers (min to max). Error bars represent the SD, statistical test used: ratio paired t-test.

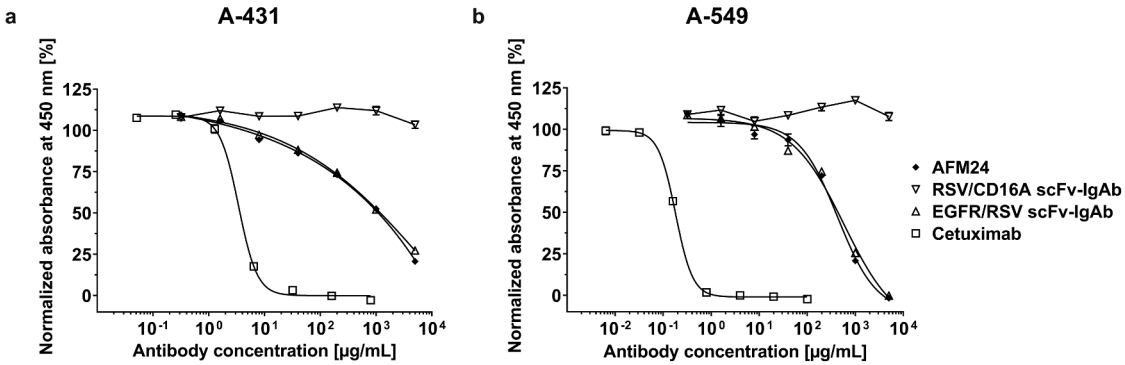

Figure 6. Inhibition of EGF-stimulated EGFR phosphorylation by AFM24. A) A-431 or B) A-549 cells were incubated with increasing concentrations of either AFM24 or comparators (RSV/CD16A scFv-IgAb, EGFR/RSV scFv-IgAb, or cetuximab) and subsequently stimulated with 100 ng/mL recombinant human EGF for 10 min at 37°C. Cell lysates were used in an ELISA for the detection of phosphorylated EGFR. Phosphorylation intensity was normalized to EGF-stimulated samples without antibody incubation. Error bars represent SD. One representative experiment is shown out of seven (for A-431) or two (A-549) performed.

the tested AFM24 dose level between 8 and 75 mg/kg/week (Supplementary Table S4). After reaching C_{max}, AFM24 serum concentrations declined, with mean half-life ($t_{1/2}$) values ranging from 32.1 to 94 hours on Day 1 found to be in the range of cetuximab and panitumumab (Supplementary Table S4). Mean AFM24 serum levels are depicted in a log-linear plot (Supplementary Figure S5). No substantial accumulation of AFM24 was observed after 5 once-weekly doses (Supplementary Table S4). Anti-drug antibody (ADA) screening was conducted to determine whether ADAs were affecting the pharmacokinetics of AFM24. ADA-positive results were reported for 10/26 AFM24-treated animals. Eight of 10 animals revealed no effect on AFM24 exposure; only two animals in Group 3 (24 mg/kg) with a strong anti-drug response revealed substantially reduced exposure, consistent with ADA-mediated clearance of AFM24.

In summary, AFM24 was well tolerated up to the highest dose level (75 mg/kg) and no skin and organ toxicity was observed. The no observed adverse effect level (NOAEL) was considered 75 mg/kg under the conditions of this study.

AFM24-induced cytokine release and other pharmacodynamic effects in cynomolgus monkeys

As shown in Figure 7a, AFM24 had a temporary effect on IL-6 serum levels within 2 hours in all animals after the first administration in comparison to the vehicle-treated group. The highest levels observed were 602 pg/mL for one female at 24 mg/kg and 416 pg/mL for a female at 75 mg/kg. IL-6 levels returned to baseline within 24 hours and were most likely triggered by the expected pharmacology of AFM24. No clear dose-dependency was observed. Analysis of other cytokines revealed that AFM24 did not affect IL-2, interferon (IFN)-γ, and tumor necrosis factor (TNF) levels after the first dose. Immunophenotyping of the peripheral blood revealed a slight and transient reduction in absolute NK cell counts ($CD3^-/CD20^-/CD159a^+$) at a dose ≥8 mg/kg, 4 hours after dosing on Day 1 for animals of both genders. This effect was not present for the control group and returned to the range of pre-dose levels (for almost all animals) until Day 8 (Figure 7b). In addition, we observed an increase in absolute $CD14^+$ monocyte counts 4 hours after the first dose in all AFM24-treated groups that was not dose-dependent.The observation is considered as AFM24-related because control data from the vehicle group were within normal variability (Figure 7c).

AFM24-induced cytokine release in human PBMC in vitro

To assess AFM24-mediated release of various cytokines *in vitro*, primary human PBMC from healthy donors were incubated in the presence of EGFR-positive human A-431 tumor target cells with increasing concentrations of AFM24 (Figure 7d). A release of IL-6, TNF, and IFN-γ could be detected in the cell culture supernatants after 24 hours of incubation in the presence of A-431 tumor target cells (Figure 7d). Highest potency values (mean EC_{50}, 29.5 pM), and highest maximal efficacy (mean E_{max}, 723.0 pg/mL) for AFM24-triggered release were observed for IL-6, demonstrating that proinflammatory IL-6 was the most prominent cytokine released (Figure 7d). This finding is in line with the elevated IL-6 levels observed in the cynomolgus monkey toxicity study (Figure 7a). The mean EC_{50} and E_{max} values for TNF release were 248.9 pM and 183.7 pg/mL, respectively, and the mean EC_{50} and E_{max} values for AFM24-stimulated IFN-γ release were 156.8 pM and 42.1 pg/mL, respectively (Figure 7d). In summary, AFM24 was found to stimulate the release of IL-6, TNF, and IFN-γ in a concentration-dependent manner and in the presence of A-431 target cells (Figure 7d).

Discussion

AFM24 was developed by the fit-for-purpose ROCK® platform by screening a library of scFv derived from human PBMCs. Unique CD16A-specific antibody variable domains were then selected and optimized for affinity and avidity aimed at sustainable activation of the innate immune system, including NK cells and macrophages.[43] AFM24's architecture is the same IgG-like format as a scFv-IgG, which in principle is an extended human IgG_1 molecule with two EGFR-binding moieties fused to the C-terminus and anti-CD16A variable fragments (Fv) within both antigen-binding arms of the antibody. AFM24 demonstrates high-affinity binding to CD16A expressed on human NK cells and macrophages. AFM24's binding characteristics to CD16A are unique with regard to: (1) binding

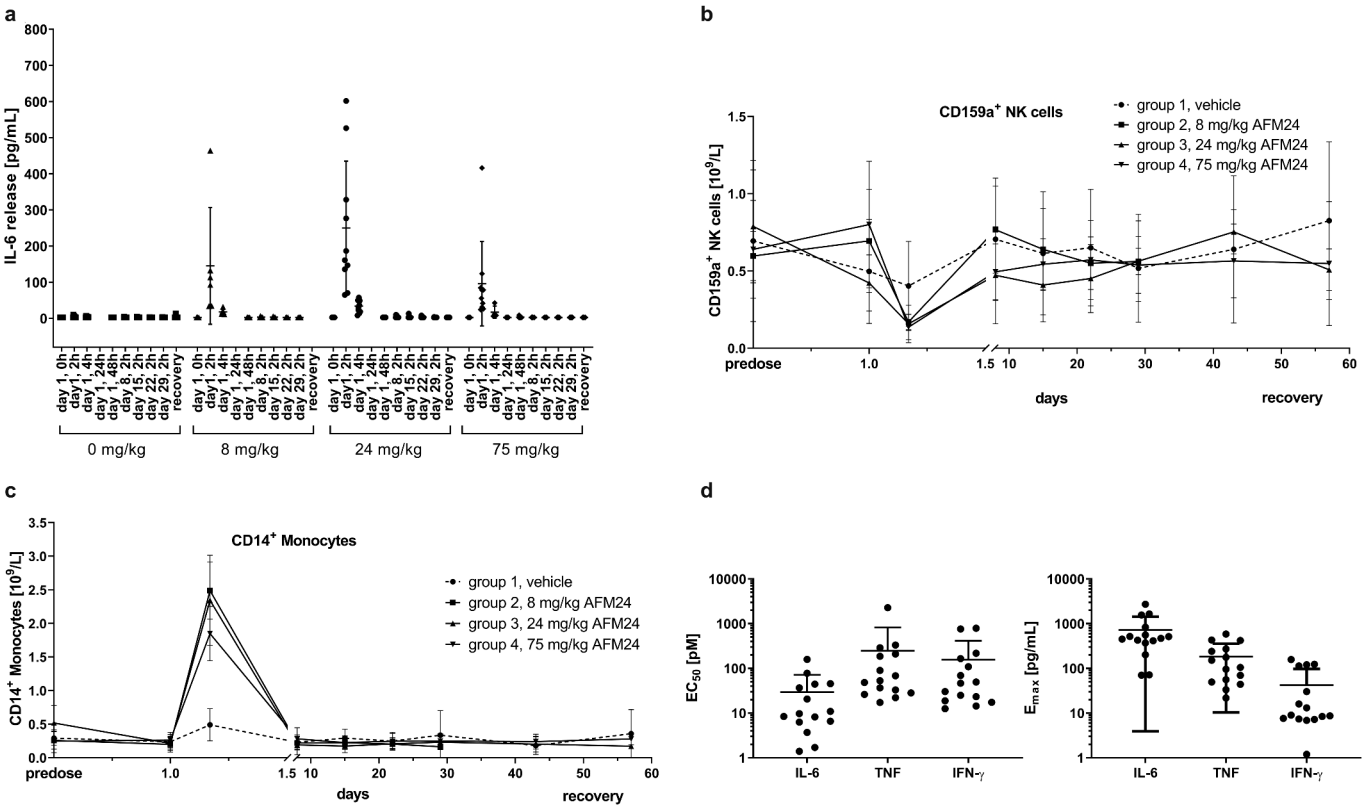

Figure 7. AFM24-induced cytokine release (*in vitro* and *in vivo*) and pharmacodynamic effect in cynomolgus monkeys. A) IL-6 release induced in cynomolgus monkeys during repeated weekly i.v. dosing of AFM24 at three dose levels and vehicle control. Time points are indicated in hours after start of infusion. Scatter plot includes mean and SD. B) $CD3^-/CD20^-/CD159a^+$ NK cells and C) $CD14^+$ monocytes were quantified in peripheral blood by flow cytometry. EDTA blood samples were withdrawn from all animals once during the pre-dose phase; on Days 1 (pre-dose and 4 hours post-dose), 8, 15, 22, and 29 (pre-dose) of the dosing phase; and from all animals on Days 14 and 28 of the recovery phase. D) Human PBMC were cultured in the presence of EGFR-positive A-431 cells at an E:T ratio of 50:1 with or without increasing concentrations of AFM24. Following a 24-hour incubation, the levels of IL-6, TNF, and IFN-γ were quantified in the cell culture supernatants. EC_{50} and E_{max} of cytokine release were determined by non-linear regression in independent experiments. Data points (n = 15) were collected in 8 independent experiments with PBMC from 10 different donors and 4 different batches of AFM24. Scatter plots show individual experiments as dots, mean, and SD.

affinity, and (2) CD16A binding epitope compared to the Fc region of IgGs, as demonstrated by sustained NK cell binding and ADCC of AFM24 in the presence of competing IgG. In contrast to monoclonal antibodies, high affinity binding of ROCK® engagers to CD16A on NK cells has been observed irrespective of the CD16A allotype as previously reported,[40,43] which may add clinical benefit for patient populations carrying the low affinity CD16A 158 F allele at position 158.[46,47]

NK cell-dependent ADCC has been reported as a MOA for mAbs, including cetuximab.[14,48] Higher EGFR expression was accompanied by inefficient cetuximab-dependent inhibition of signal transduction, but significant ADCC activity by NK cells, which is in contrast to the inhibition of EGF-induced phosphorylation as the predominate MOA in low EGFR-expressing tumors *in vitro*.[15] We show that AFM24 is potent and effective at mediating ADCC in the low picomolar range, regardless of EGFR expression on the tumor target cell. The potency and efficacy of ADCC did not correlate with the EGFR expression level: low potencies were determined on MCF-7 cells expressing very low EGFR levels. These findings strongly suggest that tumors expressing very low or heterogenous expression levels of EGFR can be effectively targeted, and that factors other than EGFR surface levels contribute to the susceptibility of tumor cells to AFM24-mediated ADCC. In contrast to the lack of correlation between potency and efficacy in ADCC and EGFR expression level, the apparent AFM24 affinity to target cells correlates well with EGFR expression levels. This may be explained by AFM24's ability to engage and activate one NK cell by binding to two CD16A receptor molecules while binding monovalent to target cells, and thereby AFM24 enables efficacious NK cell activation and cytotoxicity despite low EGFR expression levels on the target cell. In addition, AFM24 is able to mediate ADCC in the presence of high concentrations of human IgG with minimal competition. Macrophage-mediated ADCP is a putative mechanism of tumor clearance by therapeutic antibodies.[33,34] AFM24 induced efficient phagocytosis of tumor target cells with various EGFR expression levels, whereas cetuximab, representing a classical IgG_1, was found to be inefficient at ADCP with low and intermediate EGFR-expressing target cells. Altogether, these data demonstrate that AFM24 has the potential to mediate potent effector functions (ADCC and ADCP) in the tumor bed in the presence of competing IgG and irrespective of EGFR expression levels, and differentiate AFM24 from currently marketed anti-EGFR monoclonal antibodies, which have MOA that critically rely on inhibition of EGFR signal transduction.

EGFR-targeting drugs are also limited in their clinical use because of the mutational status of the EGFR signal transduction cascade. Inhibition of signal transduction of cetuximab has been shown to be ineffective in ~40% of CRC patients carrying KRAS mutations.[11] Importantly, the primary MOA of AFM24 does not depend on the mutational status of the

target cell, as demonstrated by AFM24-induced ADCC toward tumor cells harboring different intrinsic or acquired mutations that have been shown to be associated with anti-EGFR treatment resistance.[49,50] These data indicate the potential therapeutic benefit of AFM24 in cancers with KRAS, BRAF, or tyrosine kinase mutations.

Anti-EGFR therapy results in a significant benefit for cancer patients, e.g., HNSCC, when applied either alone or in combination with radiation therapy or chemotherapy.[51,52] However, many patients experience adverse events that, in some cases necessitate dose reduction or termination of therapy.[45] The most common side effects of EGFR-targeted therapies are skin toxicities and diarrhea.[45] Blockade of the EGFR pathway enhances skin inflammation via antigen presentation of skin keratinocytes, potentially to autoreactive T cells, a putative mechanism of EGFR-induced skin rash.[53,54] Different reports suggest that dose modifications or interruptions as a result of skin toxicity occur in as often as ~30% of patients.[55] The modest inhibition of EGFR signal transduction by AFM24 (~1000-fold less potent when compared to cetuximab), may potentially result in a superior clinical safety profile for AFM24 compared to cetuximab, particularly with respect to skin toxicity. Toxicity studies in cynomolgus monkey further support these assumptions; AFM24 was well-tolerated in cynomolgus monkeys up to 75 mg/kg with no skin and organ toxicity. A transient elevation of serum IL-6 levels at all dose levels was observed 2–4 hours post dose and was fully reversible after 24 hours, indicating a transient pharmacodynamic effect of AFM24. In stark contrast, historical data from cetuximab in cynomolgus monkey toxicity studies (study design and weekly dosing similar to the studies described here) demonstrated more severe skin toxicity and other toxicities at 75 mg/kg, with a striking 50% mortality rate due to sepsis.[56] Dose-dependent mean half-lives determined for AFM24 (Day 1, 32–94 hours; Day 29, 67–79 hours) were found to be in the range of cetuximab and panitumumab (Supplementary Table S4).

The pharmacological activity of AFM24 is characterized by inducing NK cell-mediated ADCC activity and macrophage-mediated ADCP. In cynomolgus monkeys, immune cell activity was potentially indicated by: (1) transient elevation of circulating IL-6 levels at all dose levels 2–4 hours after the first dose; (2) a transient reduction in absolute NK cell counts at a dose ≥8 mg/kg 4 hours after dosing on Day 1 for animals of both genders, which was not present for the control group and returned for almost all animals to the range of pre-dose data until Day 8; and (3) an increase in absolute $CD14^+$ monocyte counts at 4 hours after the first dose in all dose groups. Taken together, our data demonstrate that AFM24 could be a potentially effective treatment option associated with less pronounced EGFR-related toxicities. Based on these preclinical analyses, a first-in-human Phase 1/2a study (NCT04259450) of AFM24 for the treatment of EGFR-expressing cancers has been initiated and is currently enrolling patients.

In conclusion, currently marketed EGFR-targeting mAbs (e.g., cetuximab, panitumumab) and TKIs (e.g., erlotinib, gefitinib, osimertinib) primarily work by inhibiting EGFR-phosphorylation and are approved in CRC, HNSCC, and NSCLC only. In these cancers, the drugs show good clinical efficacy, but they are associated with toxicities (e.g., skin, organs) and are susceptible to the occurrence of primary and secondary resistance mechanisms of the EGFR-signaling cascade, which limits their use in cancer patients. Here, we characterize the functionality of AFM24 as a bispecific innate cell engager with a potentially unique modality of tumor cell elimination by innate immune cells, namely NK cells and macrophages, via ADCC and ADCP, respectively. AFM24 was found to be safe *in vivo* and with a favorable tolerability. With the described characteristics, AFM24 potentially addresses a high unmet medical need for alternate therapeutic options across various EGFR-positive tumors, with a potentially favorable tolerability profile and the ability to overcome intrinsic and acquired resistance mechanisms.

Materials and Methods

Antibody reagents and antigens

AFM24 was designed as a tetravalent bispecific IgG_1-scFv fusion antibody (scFv-IgAb) specific for human EGFR and human CD16A. Variable heavy and light-chain domains of an antibody with specificity for CD16A (clone LSIV21)[40] were fused at their C-terminus to CH1 and CL of effector-silent human IgG_1 respectively.[57] VH and VL of EGFR-specific antibody 21 were fused to the C-terminus of CH3 in scFv format using a $(GGGGS)_2$ connector. Expression vectors were cloned as previously described.[43] Recombinant antibodies, soluble or cell surface-anchored antigens were expressed in Chinese hamster ovary cells as previously described.[58] AFM24 was purified as previously described.[59] The indicated antibodies were chemically biotinylated using Biotin-X-NHS Protein Labeling Kit (Jena Bioscience, cat.: FP-321) according to the manufacturer's instructions.

Cell lines and cell culture

Detroit 562 (CCL-138), Panc 08.13 (CRL-2551), SCC-25 (CRL-1628), and SW-982 (HTB-93) were purchased from ATCC, A-549 (ACC 107), DK-MG (ACC 277), HCT-116 (ACC-581), KARPAS-299 (ACC 31), and MDA-MB-231 (ACC 732) from DSMZ (Braunschweig, Germany). A-431, COLO205, HT-29, LoVo, and MCF-7 were provided by Dr. G. Moldenhauer (DKFZ, Heidelberg, Germany). Cells were cultured as previously described.[43]

Isolation of PBMC and enrichment of human NK cells and differentiation of macrophages

PBMC and NK cells were isolated from the buffy coats of blood from healthy volunteers, as previously described.[40] For macrophage differentiation, PBMC were discarded after overnight (O/N) culture while adherent mononuclear cells were used for subsequent differentiation protocol. Complete RPMI 1640 supplemented with human M-CSF (50 ng/mL final, Gibco, cat.: PHC9501) was added to monocytes and replenished every 5–6 days. Depending on cell morphology, density, and growth, adherent macrophages were harvested after 1–4 weeks using accutase (Corning, cat. 25–058-Cl) treatment for subsequent analyses.

Cell binding assays and flow cytometric analysis

Aliquots of 0.2–1 × 10^6 of the indicated cells were incubated with 100 µL of serial dilutions of the indicated antibody constructs in fluorescence-activated cell sorting (FACS) buffer (phosphate-buffered saline (PBS), Invitrogen, cat.: 14190–169) containing 2% heat-inactivated fetal calf serum (Invitrogen, cat.: 10270–106) and 0.1% sodium azide (Roth, cat.: A1430.0100) in the absence or, if indicated, in the presence of 10 mg/mL polyclonal human IgG (Gammanorm, Octapharma) for 45 min at 37°C. After repeated washing with FACS buffer, AFM24 bound to $EGFR^+$ tumor cells was detected with 15 µg/mL fluorescein isothiocyanate (FITC)-conjugated goat anti-human IgG Fc (Dianova, cat.: 109–095-098). On NK cells and macrophages, AFM24 was detected with 10 µg/mL anti-AFM24 mAb followed by 15 µg/mL FITC-conjugated goat anti-mouse IgG (Dianova, cat.: 115–095-062). Cell surface bound biotinylated IgG were detected with 2 µg/mL Streptavidin-DyLight 488 (Dianova, cat.: 016–480-084). All incubations with secondary reagents and washing steps were performed on ice. After the last staining step, the cells were washed again and resuspended in 0.2 mL of FACS buffer containing 2 µg/mL propidium iodide (Sigma, cat.: P4170) in order to exclude dead cells. The fluorescence of 2–5 × 10^3 living cells was measured using CytoFlex or CytoFlexS flow cytometers (Beckman Coulter, Krefeld, Germany), and the median fluorescence intensities of the cell samples were determined. After subtracting the fluorescence intensity values of the cells stained with the secondary and/or tertiary reagents alone, the values were used for nonlinear regression analysis. Equilibrium dissociation constants (K_D) were calculated using the one-site-binding (hyperbolic) fit and GraphPad Prism software version 9 (GraphPad Software, La Jolla, California USA).

EGFR expression on cell lines was quantified using 10 µg/mL anti-EGFR mAb H11 (Dianova, cat. DLN-08919) and QIFIKIT (DAKO, cat.: K0078), followed by $F(ab')_2$ fragment of FITC-conjugate goat anti-mouse IgG according to the manufacturer's instructions. Samples were analyzed using CytoFlex or CytoFlexS flow cytometers (Beckman Coulter, Krefeld, Germany).

EGFR binding and competition in ELISA

96-well ELISA plates (Immuno Maxisorp, Nunc) were coated overnight at 4°C with recombinant EGFR fused to human Fc at a concentration of 3 µg/mL in 100 mM carbonate-bicarbonate buffer. After blocking with 3% (w/v) skimmed milk powder (Sigma) dissolved in PBS serial dilutions of AFM24 were incubated on the antigen coated plates with or without premixing with cetuximab in two fixed concentrations and incubated for 1.5 h at room temperature. After washing three times with 300 µL per well of PBS containing 0.1% (v/v) Tween 20, plates were incubated with anti-AFM24 mAb for 1 h followed by washing and detection with peroxidase-conjugated goat anti-mouse IgG (Dianova, cat.: 115–035-071) at 1:10,000 dilution for 1 h at room temperature. After washing, plates were incubated with tetramethylbenzidine substrate (Seramun) for 1–2 min. Reaction was stopped by addition of 0.5 M H_2SO_4 (100 µL/well). Absorbance was measured at 450 nm, 100 flashes using a multiwell plate reader (Ensight, Perkin Elmer). Mean and standard deviation of absorbance values of duplicates were plotted and analyzed using GraphPad Prism version 9.

In vitro ADCP and ADCC assay

In vitro calcein-release assays for measuring ADCC were performed as previously described.[43] For ADCP, macrophages were seeded in 96-well UpCell plates (Thermo Fisher Scientific, cat.: 174897) and cultured O/N. Target cells were labeled with 0.5 µM CellTracker™ Green CMFDA Dye (Thermo Fisher Scientific, cat.: C2925) at 37°C for 30 min, washed, and cultured O/N. Target cells were seeded on top of the macrophages (E:T ratio of 5:1), and the indicated antibodies were added at serial concentrations (0.3 pg/mL – 30 µg/mL) in duplicates. After 4 hours incubation, cells were detached from the culture plate by incubation on ice and stained with A700-labeled anti-CD11b (M1/70; BioLegend, cat.: 101222) and fixable viability dye eF780 (Thermo Fisher Scientific, cat.: 65–0865-14) for 30 min at 4°C. Phagocytosis of labeled target cells was quantified by analyzing $CMFDA^+$/$CD11b^+$ cells in % of viable cells by flow cytometry. ADCP in absence of antibodies was assessed in duplicates.

EGFR phosphorylation assay

A-431 or A-549 cells were seeded in 96-well plates in complete Dulbecco's Modified Eagle Medium (DMEM) and cultured for 20–22 h. Cells were starved for 4 hours in DMEM before 30 min incubation with serial dilutions of the indicated antibodies. EGF (100 ng/mL; Thermo Fisher Scientific, cat.: 10605-HNAE-250) was added for 10 min at 37°C before cells were washed with ice-cold PBS, lysed and used for relative quantification of phosphorylated EGFR using a Phospho-EGFR ELISA Kit (enzyme-linked immunosorbent assays, RayBiotech, cat.: PEL-EGFR-Y) according to the manufacturer's instructions.

In vitro cytokine release assay

Analysis was performed as previously described.[43]

Toxicology study in cynomolgus monkeys

Cynomolgus monkey studies were conducted at COVANCE (Münster, Germany). Purpose-bred cynomolgus monkeys (Macaca fascicularis) of Mauritian origin were selected to provide 18 healthy animals of each sex. AFM24 was formulated in 0.9% sodium chloride and administered intravenously (2 hours, chair-restrained), once weekly on Days 1, 8, 15, 22, and 29 of the dosing phase. Assessment of toxicity was based on clinical observations, body weights, food consumption, body temperature, cardiovascular investigations, ophthalmology, clinical pathology, blood immunophenotyping, and cytokine analysis. Complete necropsies were performed on all animals, with a recording of macroscopic abnormalities for all tissues. Organ weights and microscopic examinations were conducted. In addition, blood was collected for toxicokinetic and ADA analyses.

Quantification of cytokines in cynomolgus monkey serum

Blood samples for the determination of cytokine levels (IL-2, IL-6, IL-8, TNF, IFN-γ) were collected on Day 1 before start of infusion and 2, 4, 24, and 48 hours after start of infusion. On Days 8, 15, 22, and 29 and the last week of recovery, blood was collected 2 hours after start of infusion. Cytokine concentrations were determined using EMD Millipore Multiplex MAP kit on a Luminex® 200TM (MILLIPLEX MAP Non-Human Primate Cytokine Magnetic Bead Panel – Immunology Multiplex Assay, cat.: PCYTMG-40 K-PX23) using a validated method.

Pharmacokinetic analysis of AFM24

For the assessment of pharmacokinetic parameters of AFM24 in cynomolgus monkey serum, samples were collected on Day 1 pre-dose, 2, 4, 24 and 48 hours after commencement of infusion. On Days 8, 15, 22, and 29, blood was collected pre-dose and 2 hours after the start of infusion. From recovery animals, blood was withdrawn 5 minutes after infusion, and 0.5, 2, 8, 24, 48, 96, 168, 336, 504, and 672 hours after finalization of infusion. Serum bioanalysis was conducted using a validated electrochemiluminescence immuno-assay method to quantify AFM24 in cynomolgus monkey serum. The lower limit of quantitation for the method was 80 ng/mL. Pharmacokinetic interpretation was conducted by COVANCE (Harrogate) using non-compartmental methods computed with Phoenix WinNonlin (Certara USA, Inc.).

Antidrug antibody assay

Serum bioanalysis was conducted using a validated electrochemiluminescent bridging immunoassay method. The method used a floating cutpoint established from naive cynomolgus monkey serum samples. The sensitivity of the method, defined as the lowest concentration of positive control ADA that consistently provides signals above the cutpoint was 500 ng/mL in undiluted serum.

Statistical analyses

Graphical display and statistical analyses of data were performed using GraphPad Prism. Correlation between SABC and EC_{50}, E_{max}, or K_D values was analyzed using Spearman's rank correlation (nonparametric measure of rank correlation). Statistical significance was defined by p values ≤0.05. Statistical significance was calculated with ratio paired tests, if not otherwise stated. K_D values were calculated using the one-site-binding (hyperbolic) fit and GraphPad Prism software. If possible, fitting of the non-linear regression model to sigmoidal dose–response curves (variable slope) using GraphPad Prism was conducted. Statistical analysis of flow cytometry data obtained from cynomolgus monkey peripheral blood was performed by pairwise comparisons of each treated group against the control group. Tests were performed using a two-sided risk test.

Acknowledgments

This study was supported by Affimed GmbH. We thank Dacia Chase PhD and John Facciponte PhD, from the W2O Group, for assistance in drafting, editing, and critically reviewing the manuscript. We thank Covance Laboratories GmbH (Muenster, Germany) for performing the toxicology studies in the cynomolgus monkey.

Disclosure statement

SW, UR, SK, MK, MD, JP, US, TM, IF, KE, MT, TH, JK, WF, ER are employees and hold stock options of Affimed. MT was an Affimed employee at the time of data generation.

ORCID

Torsten Haneke http://orcid.org/0000-0003-2563-1055

References

1. Herbst RS. Review of epidermal growth factor receptor biology. Int J Radiat Oncol Biol Phys. 2004;59(2):21–26. doi:10.1016/j.ijrobp.2003.11.041.
2. Stintzing S, Ivanova B, Ricard I, Jung A, Kirchner T, Tannapfel A, Juette H, Hegewisch-Becker S, Arnold D, Reinacher-Schick A. Amphiregulin (AREG) and epiregulin (EREG) gene expression as predictor for overall survival (OS) in oxaliplatin/fluoropyrimidine plus bevacizumab treated mCRC patients-analysis of the Phase III aio KRK-0207 trial. Front Oncol. 2018;8:474. doi:10.3389/fonc.2018.00474.
3. Scaltriti M, Baselga J. The epidermal growth factor receptor pathway: a model for targeted therapy. Clin Cancer Res. 2006;12(18):5268–72. doi:10.1158/1078-0432.CCR-05-1554.
4. Wieduwilt MJ, Moasser MM. The epidermal growth factor receptor family: biology driving targeted therapeutics. Cell Mol Life Sci. 2008;65(10):1566–84. doi:10.1007/s00018-008-7440-8.
5. Paz-Ares LG, Gomez-Roca C, Delord JP, Cervantes A, Markman B, Corral J, Soria JC, Berge Y, Roda D, Russell-Yarde F et al. Phase I pharmacokinetic and pharmacodynamic dose-escalation study of RG7160 (GA201), the first glycoengineered monoclonal antibody against the epidermal growth factor receptor, in patients with advanced solid tumors. J Clin Oncol. 2011;29(28):3783-3790. doi:10.1200/JCO.2011.34.8888.
6. Saltz LB, Meropol NJ, Loehrer PJ Sr., Needle MN, Kopit J, Mayer RJ. Phase II trial of cetuximab in patients with refractory colorectal cancer that expresses the epidermal growth factor receptor. J Clin Oncol. 2004;22(7):1201–08. doi:10.1200/JCO.2004.10.182.
7. Hecht JR, Patnaik A, Berlin J, Venook A, Malik I, Tchekmedyian S, Navale L, Amado RG, Meropol NJ. Panitumumab monotherapy in patients with previously treated metastatic colorectal cancer. Cancer. 2007;110(5):980–88. doi:10.1002/cncr.22915.
8. Ciardiello F, Tortora G. EGFR antagonists in cancer treatment. N Engl J Med. 2008;358(11):1160–74. doi:10.1056/NEJMra0707704.
9. Goldstein NI, Prewett M, Zuklys K, Rockwell P, Mendelsohn J. Biological efficacy of a chimeric antibody to the epidermal growth factor receptor in a human tumor xenograft model. Clin Cancer Res. 1995;1:1311–18.
10. Yang XD, Jia XC, Corvalan JR, Wang P, Davis CG, Jia XC, Corvalan JR, Wang P, Davis CG, Corvalan JR, et al. Development of ABX-EGF, a fully human anti-EGF receptor monoclonal antibody, for cancer therapy. Crit Rev Oncol Hematol. 2001;38(1):17–23. doi:10.1016/S1040-8428(00)00134-7.
11. Andreyev HJ, Norman AR, Cunningham D, Oates JR, Clarke PA. Kirsten ras mutations in patients with colorectal cancer: the multicenter "RASCAL" study. J Natl Cancer Inst. 1998;90(9):675–84. doi:10.1093/jnci/90.9.675.

12. Li T, Perez-Soler R. Skin toxicities associated with epidermal growth factor receptor inhibitors. Target Oncol. 2009;4 (2):107–19. doi:10.1007/s11523-009-0114-0.
13. Roda JM, Joshi T, Butchar JP, McAlees JW, Lehman A, Tridandapani S, Carson WE. The activation of natural killer cell effector functions by cetuximab-coated, epidermal growth factor receptor positive tumor cells is enhanced by cytokines. Clin Cancer Res. 2007;13(21):6419–28. doi:10.1158/1078-0432.CCR-07-0865.
14. Martinelli E, De Palma R, Orditura M, De Vita F, Ciardiello F. Anti-epidermal growth factor receptor monoclonal antibodies in cancer therapy. Clin Exp Immunol. 2009;158(1):1–9. doi:10.1111/j.1365-2249.2009.03992.x.
15. Derer S, Bauer P, Lohse S, Scheel AH, Berger S, Kellner C, Peipp M, Valerius T. Impact of epidermal growth factor receptor (EGFR) cell surface expression levels on effector mechanisms of EGFR antibodies. J Immunol. 2012;189(11):5230–39. doi:10.4049/jimmunol.1202037.
16. Sanseviero E. NK cell-Fc receptors advance tumor immunotherapy. J Clin Med. 2019;8(10). doi:10.3390/jcm8101667.
17. Gerdes CA, Nicolini VG, Herter S, van Puijenbroek E, Lang S, Roemmele M, Moessner E, Freytag O, Friess T, Ries CH et al. GA201 (RG7160): a novel, humanized, glycoengineered anti-EGFR antibody with enhanced ADCC and superior in vivo efficacy compared with cetuximab. Clin Cancer Res. 2013;19(5):1126–38. doi:10.1158/1078-0432.CCR-12-0989.
18. Temam S, Spicer J, Farzaneh F, Soria JC, Oppenheim D, McGurk M, Hollebecque A, Sarini J, Hussain K, Soehrman Brossard S et al. An exploratory, open-label, randomized, multicenter study to investigate the pharmacodynamics of a glycoengineered antibody (imgatuzumab) and cetuximab in patients with operable head and neck squamous cell carcinoma. Ann Oncol. 2017;28(11):2827–35. doi:10.1093/annonc/mdx489.
19. Kol A. Terwisscha van Scheltinga A, Pool M, Gerdes C, de Vries E, de Jong S. ADCC responses and blocking of EGFR-mediated signaling and cell growth by combining the anti-EGFR antibodies imgatuzumab and cetuximab in NSCLC cells. Oncotarget. 2017;8:45432–46.
20. Fiedler W, Cresta S, Schulze-Bergkamen H, De Dosso S, Weidmann J, Tessari A, Baumeister H, Danielczyk A, Dietrich B, Goletz S et al. Phase I study of tomuzotuximab, a glycoengineered therapeutic antibody against the epidermal growth factor receptor, in patients with advanced carcinomas. ESMO Open. 2018;3(2): e000303. doi:10.1136/esmoopen-2017-000303.
21. Lynch TJ, Bell DW, Sordella R, Gurubhagavatula S, Okimoto RA, Brannigan BW, Harris PL, Haserlat SM, Supko JG, Haluska FG et al. Activating mutations in the epidermal growth factor receptor underlying responsiveness of non-small-cell lung cancer to gefitinib. N Engl J Med. 2004;350(21):2129–39. doi:10.1056/NEJMoa040938.
22. Paez JG, Janne PA, Lee JC, Tracy S, Greulich H, Gabriel S, Herman P, Kaye FJ, Lindeman N, Boggon TJ et al. EGFR mutations in lung cancer: correlation with clinical response to gefitinib therapy. Science. 2004;304(5676):1497–500. doi:10.1126/science.1099314.
23. Morgillo F, Della Corte CM, Fasano M, Ciardiello F. Mechanisms of resistance to EGFR-targeted drugs: lung cancer. ESMO Open. 2016;1(3):e000060. doi:10.1136/esmoopen-2016-000060.
24. Andrews Wright NM, Goss GD. Third-generation epidermal growth factor receptor tyrosine kinase inhibitors for the treatment of non-small cell lung cancer. Transl Lung Cancer Res. 2019;8(S3): S247–S64. doi:10.21037/tlcr.2019.06.01.
25. Leonetti A, Sharma S, Minari R, Perego P, Giovannetti E, Tiseo M. Resistance mechanisms to osimertinib in EGFR-mutated non-small cell lung cancer. Br J Cancer. 2019;121(9):725–37. doi:10.1038/s41416-019-0573-8.
26. Solomon BM, Jatoi A. Rash from EGFR inhibitors: opportunities and challenges for palliation. Curr Oncol Rep. 2008;10(4):304–08. doi:10.1007/s11912-008-0048-1.
27. Lanier LL. NK cell recognition. Annu Rev Immunol. 2005;23 (1):225–74. doi:10.1146/annurev.immunol.23.021704.115526.
28. Koch J, Tesar M. Recombinant antibodies to arm cytotoxic lymphocytes in cancer immunotherapy. Transfus Med Hemother. 2017;44(5):337–50. doi:10.1159/000479981.
29. Yang M, McKay D, Pollard JW, Lewis CE. Diverse functions of macrophages in different tumor microenvironments. Cancer Res. 2018;78(19):5492–503. doi:10.1158/0008-5472.CAN-18-1367.
30. Mantovani A, Marchesi F, Malesci A, Laghi L, Allavena P. Tumour-associated macrophages as treatment targets in oncology. Nat Rev Clin Oncol. 2017;14(7):399–416. doi:10.1038/nrclinonc.2016.217.
31. Guerriero JL. Macrophages: the road less traveled, changing anticancer therapy. Trends Mol Med. 2018;24(5):472–89. doi:10.1016/j.molmed.2018.03.006.
32. Long KB, Collier AI, Beatty GL. Macrophages: key orchestrators of a tumor microenvironment defined by therapeutic resistance. Mol Immunol. 2019;110:3–12. doi:10.1016/j.molimm.2017.12.003.
33. Gul N, van Egmond M. Antibody-dependent phagocytosis of tumor cells by macrophages: A potent effector mechanism of monoclonal antibody therapy of cancer. Cancer Res. 2015;75 (23):5008–13. doi:10.1158/0008-5472.CAN-15-1330.
34. Weiskopf K, Weissman IL. Macrophages are critical effectors of antibody therapies for cancer. MAbs. 2015;7(2):303–10. doi:10.1080/19420862.2015.1011450.
35. Fehniger TA, Miller JS, Stuart RK, Cooley S, Salhotra A, Curtsinger J, Westervelt P, DiPersio JF, Hillman TM, Silver N et al. A Phase 1 trial of CNDO-109-activated natural killer cells in patients with high-risk acute myeloid leukemia. Biol Blood Marrow Transplant. 2018;24(8):1581–89. doi:10.1016/j.bbmt.2018.03.019.
36. Romee R, Rosario M, Berrien-Elliott MM, Wagner JA, Jewell BA, Schappe T, et al. Cytokine-induced memory-like natural killer cells exhibit enhanced responses against myeloid leukemia. Sci Transl Med. 20168:357ra123. 357. doi:10.1126/scitranslmed.aaf2341.
37. Liu E, Marin D, Banerjee P, Macapinlac HA, Thompson P, Basar R, Nassif Kerbauy L, Overman B, Thall P, Kaplan M et al. Use of CAR-transduced natural killer cells in CD19-positive lymphoid tumors. N Engl J Med. 2020;382(6):545–53. doi:10.1056/NEJMoa1910607.
38. Klichinsky M, Ruella M, Shestova O, Lu XM, Best A, Zeeman M, et al. "Human chimeric antigen receptor macrophages for cancer immunotherapy." Nat Biotechnol. 2020;8. doi:10.1038/s41587-020-0462-y
39. Hodgins JJ, Khan ST, Park MM, Auer RC, Killers AM. 2.0: NK cell therapies at the forefront of cancer control. J Clin Invest. 2019;129: (9):3499–510. doi:10.1172/JCI129338.
40. Reusch U, Burkhardt C, Fucek I, Le Gall F, Le Gall M, Hoffmann K, Knackmuss SH, Kiprijanov S, Little M, Zhukovsky EA. A novel tetravalent bispecific TandAb (CD30/CD16A) efficiently recruits NK cells for the lysis of CD30+ tumor cells. MAbs. 2014;6 (3):728–39. doi:10.4161/mabs.28591.
41. Rothe A, Sasse S, Topp MS, Eichenauer DA, Hummel H, Reiners KS, Dietlein M, Kuhnert G, Kessler J, Buerkle C et al. A phase 1 study of the bispecific anti-CD30/CD16A antibody construct AFM13 in patients with relapsed or refractory Hodgkin lymphoma. Blood. 2015;125(26):4024–31. doi:10.1182/blood-2014-12-614636.
42. Bartlett NL, Chen RW, Domingo-Domenech E, Forero-Torres A, Garcia-Sanz R, Armand P, Devata S, Rodriguez Izquierdo A, Lossos IS, Reeder CB et al. A Phase 1b study investigating the combination of the tetravalent bispecific NK cell engager AFM13 and pembrolizumab in patients with relapsed/refractory Hodgkin lymphoma after brentuximab vedotin failure: Updated safety and efficacy data. Blood. 2018;132(Supplement 1):1620. doi:10.1182/blood-2018-99-118506.
43. Ellwanger K, Reusch U, Fucek I, Wingert S, Ross T, Muller T, Schniegler-Mattox U, Haneke T, Rajkovic E, Koch J et al. Redirected optimized cell killing (ROCK®): a highly versatile multispecific fit-for-purpose antibody platform for engaging innate immunity. MAbs. 2019;11(5):899–918. doi:10.1080/19420862.2019.1616506.
44. Kumar SS, Price TJ, Mohyieldin O, Borg M, Townsend A, Hardingham JE. KRAS G13D Mutation and Sensitivity to

Cetuximab or Panitumumab in a Colorectal Cancer Cell Line Model. Gastrointest Cancer Res. 2014;7:23–26.
45. Holcmann M, Sibilia M. Mechanisms underlying skin disorders induced by EGFR inhibitors. Mol Cell Oncol. 2015;2(4):e1004969. doi:10.1080/23723556.2015.1004969.
46. Bibeau F, Lopez-Crapez E, Di Fiore F, Thezenas S, Ychou M, Blanchard F, Lamy A, Penault-Llorca F, Frebourg T, Michel P et al. Impact of FcγRIIa-FcγRIIIa polymorphisms and KRAS mutations on the clinical outcome of patients with metastatic colorectal cancer treated with cetuximab plus irinotecan. J Clin Oncol. 2009;27(7):1122–29. doi:10.1200/JCO.2008.18.0463.
47. Cartron G, Dacheux L, Salles G, Solal-Celigny P, Bardos P, Colombat P, Watier H. Therapeutic activity of humanized anti-CD20 monoclonal antibody and polymorphism in IgG Fc receptor FcgammaRIIIa gene. Blood. 2002;99(3):754–58. doi:10.1182/blood.V99.3.754.
48. Ashraf SQ, Nicholls AM, Wilding JL, Ntouroupi TG, Mortensen NJ, Bodmer WF. Direct and immune mediated antibody targeting of ERBB receptors in a colorectal cancer cell-line panel. Proc Natl Acad Sci U S A. 2012;109(51):21046–51. doi:10.1073/pnas.1218750110.
49. Lievre A, Bachet JB, Le Corre D, Boige V, Landi B, Emile JF, Cote JF, Tomasic G, Penna C, Ducreux M et al. KRAS mutation status is predictive of response to cetuximab therapy in colorectal cancer. Cancer Res. 2006;66(8):3992–95. doi:10.1158/0008-5472.CAN-06-0191.
50. Bray SM, Lee J, Kim ST, Hur JY, Ebert PJ, Calley JN, Wulur IH, Gopalappa T, Wong SS, Qian HR et al. Genomic characterization of intrinsic and acquired resistance to cetuximab in colorectal cancer patients. Sci Rep. 2019;9(1):15365. doi:10.1038/s41598-019-51981-5.
51. Bonner JA, Harari PM, Giralt J, Azarnia N, Shin DM, Cohen RB, Jones CU, Sur R, Raben D, Jassem J et al. Radiotherapy plus cetuximab for squamous-cell carcinoma of the head and neck. N Engl J Med. 2006;354(6):567–78. doi:10.1056/NEJMoa053422.
52. Vermorken JB, Herbst RS, Leon X, Amellal N, Baselga J. Overview of the efficacy of cetuximab in recurrent and/or metastatic squamous cell carcinoma of the head and neck in patients who previously failed platinum-based therapies. Cancer. 2008;112(12):2710–19. doi:10.1002/cncr.23442.
53. Pollack BP, Sapkota B, Cartee TV. Epidermal growth factor receptor inhibition augments the expression of MHC class I and II genes. Clin Cancer Res. 2011;17(13):4400–13. doi:10.1158/1078-0432.CCR-10-3283.
54. Im JS, Herrmann AC, Bernatchez C, Haymaker C, Molldrem JJ, Hong WK, Perez-Soler R. Immune-modulation by epidermal growth factor receptor inhibitors: Implication on anti-tumor immunity in lung cancer. PLoS One. 2016;11(7):e0160004. doi:10.1371/journal.pone.0160004.
55. Abdullah SE, Haigentz M, Jr., Piperdi B. Dermatologic toxicities from monoclonal antibodies and tyrosine kinase inhibitors against EGFR: Pathophysiology and management. Chemother Res Pract. 2012;2012:351210. doi:10.1155/2012/351210..
56. Bugelski PJ, Martin PL. Concordance of preclinical and clinical pharmacology and toxicology of therapeutic monoclonal antibodies and fusion proteins: cell surface targets. Br J Pharmacol. 2012;166(3):823–46. doi:10.1111/j.1476-5381.2011.01811.x.
57. Vidarsson G, Dekkers G, Rispens T. IgG subclasses and allotypes: from structure to effector functions. Front Immunol. 2014;5:520. doi:10.3389/fimmu.2014.00520.
58. Ellwanger K, Reusch U, Fucek I, Knackmuss S, Weichel M, Gantke T, Molkenthin V, Zhukovsky EA, Tesar M, Treder M. Highly specific and effective targeting of EGFRvIII-positive tumors with TandAb antibodies. Front Oncol. 2017;7:100. doi:10.3389/fonc.2017.00100.
59. Gantke T, Weichel M, Herbrecht C, Reusch U, Ellwanger K, Fucek I, Eser M, Muller T, Griep R, Molkenthin V et al. Trispecific antibodies for CD16A-directed NK cell engagement and dual-targeting of tumor cells. Protein Eng Des Sel. 2017;30(9):673–84. doi:10.1093/protein/gzx043.